Estimation of Relevant Mass Transfer Parameters for the Extraction of Packed Substrate Beds Using Supercritical Fluids

J. M. del Valle,* P. Napolitano, and N. Fuentes

Chemical and Bioprocess Engineering Department, Pontificia Universidad Católica de Chile, P.O. Box 306, Santiago 22, Chile

Simulations were performed on supercritical fluid extraction (SFE) of solid substrates in packed beds using a general model (Model 1) that considers both diffusion within the solid particle and convection in a supercritical fluid (SF) film surrounding each particle. Two simplified models were also used that neglected either the internal (diffusion) (Model 2) or the external (convection) resistance to mass transfer between the phases (Model 3). Results of simulations showed that all models could predict similar, smooth integral extraction plots (of recovered solute, Y, versus extraction time, t). However, some differences in residual concentration profiles (solute concentration in the solid substrate, C_s, versus axial position, z) resulted when they were compared. As an example, typical S-shaped $C_s(z)$ curves became slightly steeper when the contribution of the $1/k_f a_p$ term (external resistance to mass transfer) was neglected (Model 3) or flattened when that of $R^2/15D_m$ (internal resistance to mass transfer) was neglected (Model 2). As a result of our analysis, a multi-objective fit of experimental Y versus t curves as well as C_s versus z profiles to proposed models is suggested, so as to estimate relevant mass transfer parameters for the SFE of packed substrate beds.

Introduction

Supercritical fluid extraction (SFE) processes take advantage of special physical properties of supercritical fluids (SFs). These fluids can exert solvent liquidlike power, but they also possess excellent transport properties similar to normal gases (such as low viscosity and high diffusivity).[1] The development of SFE processes for solid substrates requires appropriate modeling of mass transfer mechanisms in packed beds.[2] Mass transfer parameters derived from data generated in a laboratory or pilot plant unit can aid in the scaling-up and design of commercial-sized processes. From a scale-up viewpoint, the most interesting mass transfer models are those based on differential mass balance equations for thin cylindrical sections of a packed bed, initially proposed by Bulley et al.[3] Recent publications using this approach include those by Cuperus et al.,[4] Roy et al.,[5] Goodarznia and Eikani,[6] and several from Reverchon's group in Italy.[7−10] To solve the aforementioned equations, both the controlling mass transfer mechanism for the particular extraction process and the equilibrium relationship for the partition of the solute between the solid matrix and the SF must be known. Many researchers[6,7,10] assume a constant partition coefficient ($K = C_f/C_s$, where C_f is the solute concentration in the SF and C_s is the solute concentration in the solid). Perrut et al.[9] also assumed a constant partition coefficient but only for solute concentrations in the supercritical phase below a saturation value. Goto et al.[11] have proposed a more complex sorption isotherm to describe the equilibrium between phases.

Several authors have utilized a model that assumed external control of mass transfer rates, thus determining "volumetric" mass transfer coefficients for the extraction of canola oil,[3,12] *Dimorphoteca pluvialis* oil,[4] sunflower oil,[9] and clove bud essential oil[10] with supercritical CO_2 (SCO_2). Others have assumed internal control of mass transfer rates for the extraction of essential oil from sage[8] and essential oils and triglycerides from several sources[7] using SCO_2. The authors in last case (internal control) also assumed that the residual concentration profile within the solid matrix was parabolic in shape so as to simplify the mathematical solution of the problem. They ended up determining internal mass transfer coefficients instead of apparent diffusion coefficients to describe extraction rates. Goodarznia and Eikani[6] proposed a more general model that considered both solute diffusion within the solid and external resistance to mass transfer, together with concentration-gradient-driven axial dispersion of the solute in the supercritical phase within the bed. This model is the basis of the one used in our work.

It is worth mentioning that critical comparisons between models proposed by several research groups are lacking in the published literature. To our knowledge, only Poletto and Reverchon[7] compared two simplifications of a model that assumed internal control of extraction rates. This has important implications, because the integral extraction plot has such a simple shape that it may not allow an estimation of mass transfer parameters with significance.[2] On the other hand, residual concentration profiles on treated substrates have seldom been used for mass transfer modeling purposes.[12]

The main objetive of this work was to propose a multiobjective fitting procedure that considers both integral extraction data and residual concentration profiles of solute in a bed of treated material, so as to determine mass transfer parameters that are relevant to the extraction process. As part of our work, we analyzed the effect of phase equilibria and mass transfer factors on extraction rates determined by a general model consid-

* Corresponding author. Fax: (562) 6865803. E-mail: delvalle@ing.puc.cl.

10.1021/ie000034f CCC: $19.00
Published on Web 11/15/2000

ering mass transfer resistances in both the solid matrix and the fluid film surrounding each particle and determined situations in which simplified models neglecting one of these resistances can be applied.

Mathematical Models

We modeled a system in which a constant volumetric flow rate (F) of SF was passed through an extractor whose internal height and diameter are H and d_e, respectively. The most general model (Model 1) implemented in this work was a simplification of that proposed by Goodarznia and Eikani[6] that neglected the axial dispersion of solute in the supercritical phase. It also assumed spherical geometry of solid particles (radius R), plug flow pattern of SF (or constant interstitial velocity in the bed, u), constant physical properties of the SF and substrate in the bed, negligible pressure drops and temperature gradients in the bed, and a constant partition coefficient of the solute between the solid and supercritical phases. As a result of these asumptions, the solute concentration in the solid matrix (C_s) depends on the extraction time (t), the axial position along the bed (z), and the radial position within the particle (r), whereas the solute concentration in the SF (C_f) depends only on t and z. The differential mass balance equation in a SF film surrounding each particle was

$$\epsilon\left(\frac{\partial C_f}{\partial t} + u\frac{\partial C_f}{\partial z}\right) = (1-\epsilon)J \tag{1a}$$

where

$$J = k_f a_p (C_{fs} - C_f) \tag{1b}$$

In eqs 1a and 1b, ϵ is the void fraction of the bed, J is the amount of solute transferred from the solid substrate to the SF per unit volume of the bed, k_f is the external mass transfer coefficient, $a_p = 3/R$ is the specific surface (total surface per unit volume) of spherical particles, and $C_{fs} = KC_s|_R$ is the solute concentration in the SF at the particle surface. The equation for diffusion within the solid particle was

$$\frac{\partial C_s}{\partial t} = \frac{D_m}{r^2}\frac{\partial}{\partial r}\left(r^2\frac{\partial C_s}{\partial r}\right) \tag{2}$$

where D_m is the solute diffusivity in solid phase. The initial and border conditions for eqs 1 and 2 were

$$C_f(z,0) = C_{fo} \quad (0 \le z \le H) \tag{3a}$$

$$C_f(0,t) = 0 \quad (t \ge 0) \tag{3b}$$

$$C_s(r,0) = C_{so} \quad (0 \le r \le R) \tag{3c}$$

$$\left.\frac{\partial C_s}{\partial r}\right|_0 = 0 \quad (t \ge 0) \tag{3d}$$

$$-D_m\left.\frac{\partial C_s}{\partial r}\right|_R = k_f(C_{fs} - C_f) \quad (t \ge 0) \tag{3e}$$

In addition, two simplifications of the general model were implemented. Model 2 neglected the internal (diffusion) resistance to mass transfer. Under this asumption, there is no gradient in solute concentration within a solid particle, so that $\bar{C}_s$ (average residual solute concentration) depends only on t and z. In this particular case, eqs 1a and 1b apply but eq 2 becomes

$$\frac{\partial \bar{C}_s}{\partial t} = -k_f a_p(\bar{C}_s - C_f) \tag{4}$$

The initial and border conditions in this particular case were: $C_f(z,0) = C_{fo}$, $C_f(0,t) = 0$, and $\bar{C}_s(z,0) = C_{so}$ ($0 \le z \le H$, $t \ge 0$).

Finally, Model 3 neglected the external (convection) resistance to mass transfer. Under this asumption, the solute concentration on the particle suface, $C_s|_R$, is the one that satisfies the equilibrium relationship with the bulk of the fluid phase. In this particular case, eqs 1a and 2 apply and eq 1b becomes

$$J = -D_m a_p \left.\frac{\partial C_s}{\partial r}\right|_R \tag{5}$$

The initial and border conditions in this last case were: $C_f(0) = C_{fo}$, $C_s(r,0) = C_{so}$, $\partial C_s/\partial r|_0 = 0$ ($t \ge 0$), and $C_s|_R = C_f/K$ ($t \ge 0$).

General solutions to these systems of differential equations were obtained by resorting to the use of dimensionless numbers. These included a dimensionless time (θ, eq 6a), dimensionless position within a solid particle (ρ, eq 6b), dimensionless position along the bed (ξ, eq 6c), dimensionless solute concentration in the solid substrate (x, eq 6d), and dimensionless solute concentration in the SF (y, eq 6e), that were defined as

$$\theta = \frac{tu}{H} \tag{6a}$$

$$\rho = \frac{r}{R} \tag{6b}$$

$$\xi = \frac{z}{H} \tag{6c}$$

$$x = \frac{C_s}{C_{so}} \tag{6d}$$

$$y = \frac{C_f}{C_{fo}} \tag{6e}$$

As an example, the use of the aforementioned definitions, together with the linear equilibrium relationship ($C_{fs} = C_s|_R/K$), yielded the following system of dimensionless differential equations in the case of Model 1 (to replace eqs 1 and 2):

$$\frac{\partial y}{\partial \theta} + \frac{\partial y}{\partial \xi} = \frac{1}{\Gamma\Theta}(x|_1 - y) \tag{7}$$

$$\frac{\partial x}{\partial \theta} = \frac{1}{\tau_{int}\rho^2}\frac{\partial}{\partial \rho}\left(\rho^2\frac{\partial x}{\partial \rho}\right) \tag{8}$$

subject to the following dimensionless initial an border conditions (equivalent to eqs 3):

$$y(\xi,0) = 1 \quad (0 \le \xi \le 1) \tag{9a}$$

$$y(0,\theta) = 0 \quad (\theta \ge 0) \tag{9b}$$

$$x(\rho,0) = 1 \quad (0 \le \rho \le 1) \tag{9c}$$

$$\left.\frac{\partial x}{\partial \rho}\right|_0 = 0 \quad (\theta \ge 0) \tag{9d}$$

$$-\left.\frac{\partial x}{\partial \rho}\right|_1 = \frac{1}{3\Theta\tau_{int}}(x|_1 - y) \quad (\theta \ge 0) \tag{9e}$$

Three dimensionless parameters were defined that aided in the interpretation of the results of our sensitivity analysis. They were

$$\Gamma = \frac{\epsilon}{1-\epsilon}K \tag{10a}$$

$$\tau_{int} = \frac{R^2}{D_m}\frac{u}{H} \tag{10b}$$

$$\Theta = \frac{1}{k_f a_p}\frac{u}{H}\frac{1}{K} \tag{10c}$$

More details about the dimensionless versions of Models 2 and 3 can be obtained from the corresponding author upon request. The dimensionless differential equations were solved using the method of finite differences. In the cases of Model 1 (eqs 7−9) and Model 3, the bed and substrate particles in it were divided into several disc- and spherical-shell-shaped volume elements, respectively. It was assumed that solute concentration in the FS in each disc-shaped element of height Δz within the bed was uniform and that each particle in a section was extracted to the same level. Because, as already stated, Model 2 considered an average solute concentration for each particle, which depended only on the axial position along the bed and extraction time, in that particular case, only the bed was subdivided in disc-shaped volume elements. Approximate values of spatial derivatives were estimated using finite differences, and the resulting temporary differential equations were numerically solved using a fourth-order Runge−Kutta method implemented in MATLAB (MathWorks, Natick, MA).

Results and Discussion

Sensitivity Analysis. The three dimensionless numbers Γ (eq 10a), τ_{int} (eq 10b) and Θ (eq 10c) grouped several variables that are related to the bed and particle geometry (a_p, H, R), the fluid dynamics (u), the bed packing (ϵ), the equilibrium between phases (K), and the mass transfer mechanisms (k_f, D_m). Of these variables, K, k_f, and D_m are normally treated as fitting parameters. Dimensionless number Γ is related to the partition of solute between the phases (SF and substrate particles) under equilibrium conditions. Dimensionless number τ_{int} has been referred to as the "internally controlled, characteristic extraction time" by Reverchon.[8] It is calculated as the ratio between a term that is proportional to the internal resistance to mass transfer (R^2/D_m) and the residence time of the SF in the extractor (H/u). Dimensionless number Θ, on the other hand, is the ratio of a dimensionless number, which, proceeding by analogy to the previous case, will be referred to as the "externally controlled, characteristic extraction time" ($\tau_{ext} = u/k_f a_p H$), and the solute partition coefficient (K). The externally controlled, characteristic extraction time can be estimated as the ratio between the external resistance to mass transfer ($1/k_f a_p$) and the residence time of the SF in the extractor.

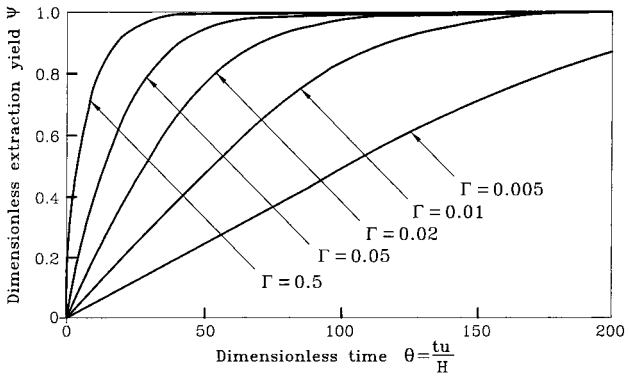

Figure 1. Effect of the partition of solute between the SF and solid particles on integral extraction plots for $\Theta = 6$ and $t_{int} = 25$ (parametric value of dimensionless number Γ indicated directly on each curve).

To analyze the effect of various parameters, integral extraction plots and residual concentration profiles were utilized in this work. For convenience, integral extraction plots were presented as graphs of dimensionless yield (Ψ, eq 11) versus dimensionless time (θ), whereas residual particle concentration profiles were presented as graphs of dimensionless concentration (x) versus dimensionless position (ξ) with θ as a parameter. Dimensionless number Ψ was defined as

$$\Psi = \frac{\Gamma}{\Gamma+1}\frac{1}{C_{fo}}\int_0^\theta C_f|_{\xi=1}\,d\theta \tag{11}$$

To carry out a sensitivity analysis a reference case was selected with $\Gamma = 0.05$, $\tau_{int} = 25$, and $\Theta = 6$. The integral extraction plots in Figure 1 clearly show that, as Γ decreases (and the solute is more tightly held by the solid matrix), the amount of solute carried out by the SF decreases, thus increasing extraction times. Figure 2 presents residual concentration profiles for $\theta = 5$ (Figure 2A) and for $\theta = 15$ (Figure 2B). Residual solute concentration profiles are clearly closer to each other, and steeper, when Γ decreases, independent of extraction time.

In our work, we analyzed simultaneous changes in τ_{int} and Θ that considered the proportion of the total resistance to mass transfer that was provided by the internal resistance in the solid substrate. Peker et al.[13] proposed that

$$\frac{\partial C_s}{\partial t} = \frac{1}{R_T}\left(\frac{\bar{C}_s}{K} - C_f\right) \tag{12a}$$

where R_T, the total resistance to mass transfer, was given by

$$R_T = \frac{(Bi+5)R}{15k_f} \tag{12b}$$

In eq 12b, $Bi = k_f R/D_m$, the dimensionless Biot number, represents the ratio between the external and internal mass transfer coefficients. In a situation of rate control

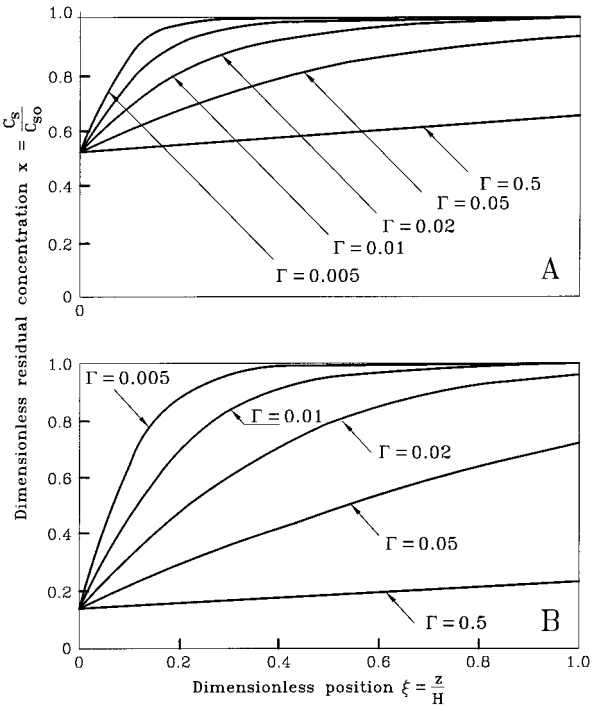

Figure 2. Effect of the partition of solute between the SF and solid particles on residual concentration profiles for $\Theta = 6$, $t_{int} = 25$, and **(A)** $\theta = 5$ or **(B)** $\theta = 15$ (parametric value of dimensionless number Γ indicated directly on each curve).

by internal mass transfer mechanisms, $k_f R \gg D_m$ and Bi + 5 ≈ Bi, whereas in a situation of rate control by external mass transfer mechanisms, $k_f R \ll D_m$ and Bi + 5 ≈ 5. Equation 12b then yields the following limits for the internal (R_{int}) and external resistance to mass transfer (R_{ext}):

$$R_{int} = \frac{R^2}{15D_m} = \frac{H\tau_{int}}{15u} \tag{13a}$$

$$R_{ext} = \frac{R}{3k_f} = \frac{KH\Theta}{u} \tag{13b}$$

In our reference case ($\Gamma = 0.05$, $\tau_{int} = 25$, $\Theta = 6$), if the porosity of the packed bed is about 60% ($\epsilon = 0.6$), then the total resistance to mass transfer is given by

$$R_T = R_{int} + R_{ext} \approx 1.867\frac{H}{u} \tag{14}$$

Figure 3 presents the effects of simultaneous changes in τ_{int} and Θ in integral extraction plots for $\Gamma = 0.05$. Selected combinations gave different values of the R_{int}/R_T ratio

$$\frac{R_{int}}{R_T} = \frac{\tau_{int}}{15K\Theta + \tau_{int}} \tag{15}$$

between 0.107 and 0.893 but were characterized by an identical value of total resistance given by eq 14. For these simulations, we assumed that the ratio H/u remains constant. It is clear from Figure 3 that, as the contribution of the internal resistance to mass transfer to the total resistance to mass transfer increases, the amount of solute carried out by the SF increased, thus decreasing extraction times. Figure 4 presents residual concentration profiles for extraction times where Ψ

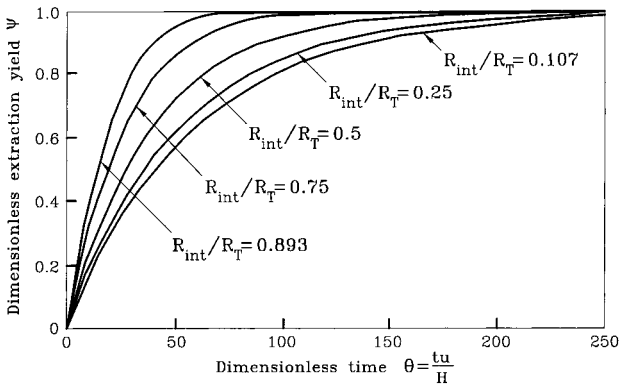

Figure 3. Effect of the ratio of internal to total resistance to mass transfer on integral extraction plots for $\Gamma = 0.05$, $\epsilon = 0.6$ and $R_T \approx 1.867H/u$ (parametric value of dimensionless ratio R_{int}/R_T indicated directly on each curve).

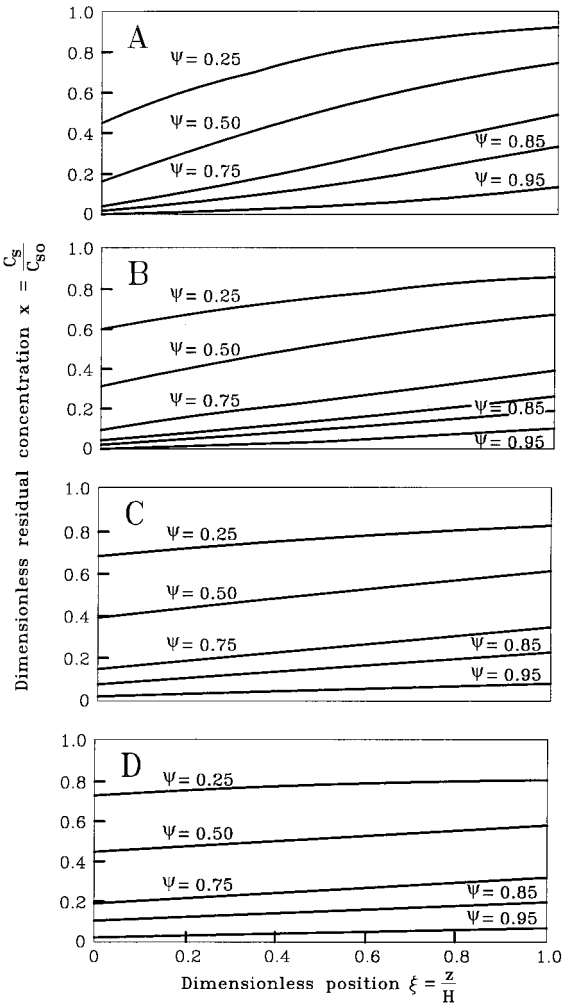

Figure 4. Effect of the ratio of internal to total resistance to mass transfer on residual concentration profiles for $\Gamma = 0.05$, $\epsilon = 0.6$, and $R_T \approx 1.867H/u$. Values of R_{int}/R_T are **(A)** 0.893, **(B)** 0.75, **(C)** 0.5, and **(D)** 0.107 (parametric value of dimensionless number Ψ indicated directly on each curve).

ranged from 0.25 to 0.95. A plot for $R_{int}/R_T = 0.25$ was omitted because it was almost superimposed on that for $R_{int}/R_T = 0.107$, so that we can assume that there is no effect of the R_{int}/R_T ratio on residual concentration profiles when $R_{int}/R_T \leq 0.25$. We can conclude from Figure 4 that an increase in the contribution of external resistance causes flatter concentration profiles of residual solute in treated substrate along the bed.

Table 1. Summary of Physical Parameters Used in Model Evaluation and Estimated Mass Transfer Parameters

	canola oil[12]		basil essential oil[16]
	(Figures 5 and 6)	(Figure 9)	(Figures 7 and 8)
	Parameters		
C_{so} [kg solute/m^3]	389.8	389.8	10.08
H [cm]	8.21	6.16	18.8
d_e [cm]	1.27	2.54	5.2
ϵ [dimensionless]	0.630	0.630	0.514
F [g CO_2/min]	2.7	1.4	20
u [mm/s]	0.65	0.08	0.46
K [g solid/g CO_2]	0.0157	0.0157	0.45
	Fitting Parameters		
$k_f a_p$ [s^{-1} × 10^2]	2.2 (Model 1) 2.0 ± 0.18 (Model 2) 3.8 (ref 16)	0.25 ± 0.01 (Model 2)[a] 0.59 ± 0.06 (Model 2)[b]	0.20 (Model 1)
D_m [m^2/s × 10^{13}]	0.47R^2 (Model 1)[c]	–	1.98 (Model 1) 2.00 ± 0.03 (Model 3) 1.50 (ref 16) 1.90 (ref 6)

[a] Value that minimized discrepancies between experimental and predicted values of $Y(t)$ (single-objective fitting procedure). [b] Value that minimized weighted discrepancies between experimental and predicted values of both $Y(t)$ and $C_s(z)$ (multi-objective fitting procedure). [c] $[R] = \mu$m.

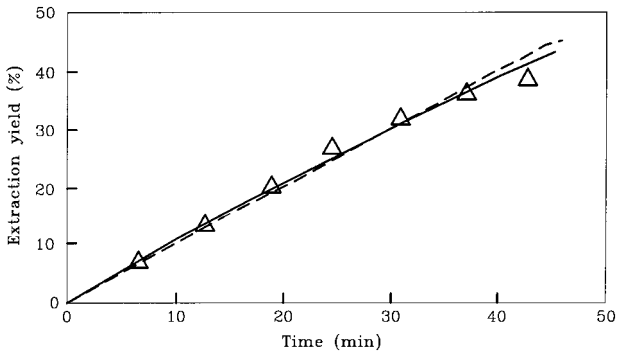

Figure 5. Fit of Model 1 (segmented line) and Model 2 (continuous line) to integral extraction data (△) reported by Lee et al.[12] for the extraction of oil from canola with supercritical carbon dioxide at 55 °C and 360 bar (Table 1).

On the basis of this sensitivity analysis, we concluded that extraction rates increased as either dimensionless number Γ increases or the mass transfer resistances decrease (τ_{int} or Θ decrease). On the other hand, the residual solute concentration profiles get steeper (more S-shaped) as either Γ decreases or the internal resistance to mass transfer makes a larger contribution to the total resistance to mass transfer.

Fitting of Experimental Data when the Internal Resistance to Mass Transfer Is Neglected. We applied Models 1 and 2 to the integral extraction data reported by Lee et al.[12] for the extraction of canola seeds with SCO_2. Fitting of model parameters (D_m and/or $k_f a_p$) to experimental data was done by minimizing the sum of squares (SS) of model residuals. Lee et al.[12] assumed that the process rate was externally controlled in this particular case, because they did not observe an effect of seed pretreatment on extraction rate. Although the treatment of the seeds prior to extraction was not clearly specified (they were apparently crushed), it is surmissed that their microstructure was considerably destroyed when a large reduction in particle size is performed so as to expose most of the oil to the solvent.[2,14] The results of our fitting excercise are presented in Figure 5, which demonstrates that both Model 1 and Model 2 can fit the experimental data equally well. Lee et al.[12] reported a value $C_f = 0.011$ g of oil/g of CO_2 for values of C_s between 0.2 and 0.7 g of oil/g of solid. Because our model considered an equilibrium relationship of the form $C_f = KC_s$, the volumetric partition coefficient (K) was estimated as $K = C_f/(C_s)_{max}$ ($K = 0.0157$ g of solid/g of CO_2). Values of other model parameters were as reported by Lee et al.[12] or calculated on the basis of information provided by the authors in their original manuscript (Table 1). Predicted values of $k_f a_p$ are also reported in Table 1. It is interesting to point out that the value $\pm 0.18 \times 10^{-2}$ s^{-1} corresponded to a 95% confidence interval for $k_f a_p$ predicted by Model 2. This confidence interval was estimated using the Monte Carlo method proposed by van Boekel.[15] After the model parameters were fit to the experimental data, a new set of synthetic data was generated by adding random errors to model predictions that had a normal distribution with a mean value of 0 and a standard deviation associated with differences between experimental values and the model predictions. New model parameters were calculated by fitting synthetic data, and this fitting procedure was reapplied several times so as to obtain a distribution of values of model parameters. This distribution allowed us to establish confidence intervals using Student's "t" stadigraph with a confidence level $(1 - \alpha/2)$ and $\nu = n - p$ degrees of freedom (n = number of data points, p = number of fitting parameters). It is also interesting to note that, in preliminary simulation runs involving Model 2, both K and $k_f a_p$ were used simultaneously as fitting parameters, and a fitted value of K was obtained that was quite similar to the assumed value (0.0181 instead of 0.0157 g of solid/g of CO_2). This gave us certain confidence on the procedure adopted to estimate K on the basis of the equilibrium information provided by Lee et al.[12]

The large difference between fitted values of external mass transfer coefficient determined by us and those reported by Lee et al.[12] may be a consequence of the different equilibrium relationships and extractor geometries assumed in each case. In fact, the value of H adopted by us (Table 1) was based on a reported value of d_e and our assumption that ϵ remained unchanged in all experiments. However, the only clear difference between our predicted integral extraction plot and that of Lee et al.[12] occurred for long extraction times (≥42 min) for which no experimental data points were provided. Indeed, we predicted a recovery of 48% of oil after 50 min of extraction with SCO_2 at 55 °C and 360

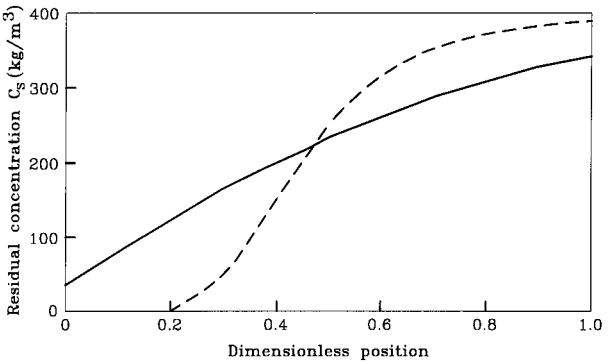

Figure 6. Residual concentration profiles predicted by Model 1 (segmented line) and Model 2 (continuous line) after 35 min of extraction (when predicted values of $Y(t)$ coincided). (Values of model parameters reported in Table 1 and Figure 5.)

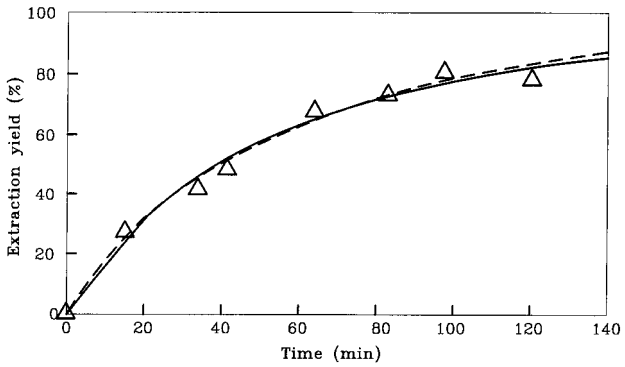

Figure 7. Fit of Model 1 (segmented line) and Model 3 (continuous line) to integral extraction data (△) reported by Reverchon et al.[16] for the extraction of essential oils from basil with supercritical carbon dioxide at 40 °C and 100 bar (Table 1).

bar, whereas Lee et al.[12] predicted a 42% recovery under the same conditions.

When the internal resistance is neglected as compared to the external resistance to mass transfer (Model 2), the numerical value for the external resistance should increase as compared to that predicted by Model 1 so as to allow a comparable yield to be attained. The small difference between the two predicted values ($1/k_f a_p$ = 44.8 s for Model 1 vs $1/k_f a_p$ = 48.9 s for Model 2) suggests that, in the case of oil extraction from crushed canola seeds, the resistance to mass transfer in the solid matrix may indeed be negligible compared to that in a presumably thick film of stagnant SF surrounding each particle. This assumption can be further sustained by comparison of fitted (Model 1) values of $1/k_f a_p$ with those of internal resistance to mass transfer ($R^2/15D_m \approx 1.5$ s; $D_m/R^2 = 4.7 \times 10^{-2}$ s^{-1}): the internal resistance is slightly above 3% of the total resistance to mass transfer.

Despite the fact that integral extraction plots predicted by Model 1 and Model 2 were virtually superimposed (Figure 5), Figure 6 demonstrates that residual concentration profiles estimated by these two models following 35 min of extraction (when predicted yields coincided) differ considerably from each other.

Fitting of Experimental Data when the External Resistance to Mass Transfer Is Neglected. We also applied Models 1 and 3 to the integral extraction data reported by Reverchon et al.[16] for the extraction of basil's essential oils with SCO_2. To do this, most model parameters were calculated on the basis of data provided either by the authors in their original manuscript or by Goodarznia and Eikani[6] (e.g., value of K), who modeled the same set of experimental data (Table 1). In this case, Reverchon et al.[16] proposed that the extraction rate was internally controlled. The authors claimed that drying and comminution ($R = 85\ \mu$m) were performed so as to avoid damage to cells in such a way that SCO_2 had to pass through an intact layer of cuticular waxes before reaching the essential oils in cell vacuoles.[17] Under these particular conditions, it is possible that solute diffusion within the solid matrix may determine the rate of extraction. The results of this fitting procedure are presented in Figure 7, which demonstrates that both Model 1 and Model 3 are able to fit the experimental data equally well. Predicted values of D_m are reported in Table 1. The 95% confidence interval for the value of D_m predicted by Model 3 ($\pm 0.03 \times 10^{-13}$ m^2/s) was determined using the Monte Carlo method, as described in the previous section.

There was a statistically significant difference between the diffusivity values fitted by Reverchon et al.[16] and us. We assumed that these were due to the differences between the stated models. Indeed, Reverchon et al.[16] proposed a concentrated parameter model in which the extraction rates of all of the particles loaded into the extractor was the same. They neglected the right-hand side term of eq 1a, which accounts for the variations in solute concentration in the SF that moves along the bed. Because the solute concentration gradients along the packed bed and outside solid substrate particles develop on different scales that are comparable to $2R$ and H, respectively, the physical phenomena responsible for the facts that both of them become negligible are not the same, and it is wrong to neglect solute concentration gradients along the bed in a situation in which internal mechanisms control mass transfer rates. This may be the result of an efficient axial dispersion of the solute or a small H/d_e ratio rather than negligible external mass transfer resistance. Moreover, Reverchon et al.[16] used film resistance values that were based on nondimensional relationships for the Sherwood's number as a function of the Reynolds' and Schmidt's numbers reported by Tan et al.[18] Statistical analysis notwithstanding, it appears that our predicted values of D_m coincided with the value reported by Goodarznia and Eikani.[6] Because the small differences may have been due to the fact that these authors included an axial dispersion term in their differential mass balance equation (eq 1a), we surmise that the contribution of axial dispersion to mass transfer may be negligible for extraction of essential oils from comminuted herbs with SCO_2 at 40 °C and 100 bar. The same conclusion was reached by Reverchon and Marrone,[10] who gathered data and modeled the extraction of essential oils from clove buds with SCO_2.

As in the previous case, it can be proposed that the internal resistance to mass transfer fitted by Model 3 (that neglects the external resistance) should be larger than that predicted by Model 1, to allow attainment of comparable yields in equivalent times. The small difference between predicted values of $R^2/15D_m$ (2457 s for Model 1 vs 2413 s for Model 3) suggests that the resistance to mass transfer in the SF film surrounding each comminuted particle may be negligible compared to that within basil leaves for SCO_2 extraction of essential oils. This assumption is further tested by comparing fitted (Model 1) values of $R^2/15D_m$ and external resistance to mass transfer ($1/k_f a_p \approx 458$ s; $k_f a_p = 0.2 \times 10^{-2}$ s^{-1}). In this particular case, the external

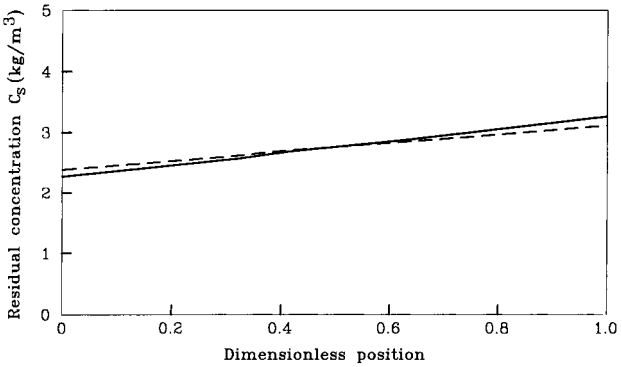

Figure 8. Residual concentration profiles predicted by Model 1 (segmented line) and Model 3 (continuous line) after 65 min of extraction (when predicted values of $Y(t)$ coincided). (Values of model parameters reported in Table 1 and Figure 7.)

resistance is slightly above 15% of the total resistance to mass transfer.

Unlike in the previous case, both the integral extraction plots predicted by Model 1 and Model 3 (Figure 7) and the residual concentration profiles estimated by these two models after 80 min of extraction time (when predicted yields coincided, Figure 8) were virtually superimposed. Only to improve clarity of presentation, the ordinate scale was limited to 0−5 kg/m^3 instead of the required full 0−10.08 kg/m^3 scale.

Multiobjetive Fitting of Experimental Data. Finally, we applied Model 2 to extraction data reported by Lee et al.[12] for the extraction of canola oil with SCO_2. In the first case, only the integral extraction data was fitted. In the second case, both the integral extraction data and the residual concentration profile data were fitted simultaneously. In this case, values of the parameters were obtained by minimizing the SS of the discrepancies between predicted and experimental values of the extraction yield, $Y(t)$, and residual solute concentration, $C_s(z)$, weighted by their respective estimated variance. This was done to account for the different magnitudes of the experimental errors in the measurements of Y and C_s. The error variance for measurements of recovered solute versus time was estimated as

$$\hat{\sigma}_Y^2 = \frac{1}{n-1}\sum_{k=1}^{n}[Y(t_k) - \hat{Y}(t_k)]^2 \qquad (17a)$$

where $Y(t_k)$ values were estimated using a single-objective optimization procedure. On the other hand, the error variance for measurements of residual solute versus position was estimated as

$$\hat{\sigma}_{C_s}^2 = \frac{1}{m-1}\sum_{k=1}^{m}[C_s(z_k) - \hat{C}_s(z_k)]^2 \qquad (17b)$$

where values of $C_s(z_k)$ were also estimated using a single objective procedure.

It is clear from Figure 9 that, despite having larger residuals for the prediction of the integral extraction curve, there is a much better fit to experimental data using the second procedure. This clearly demonstrates the advantage of applying a multi-objetive method to determine mass transfer parameters with significance. It is evident that the values of $k_f a_p$ estimated using these two methods (Table 1) differ considerably from each other. The increase in size of the 95% probability

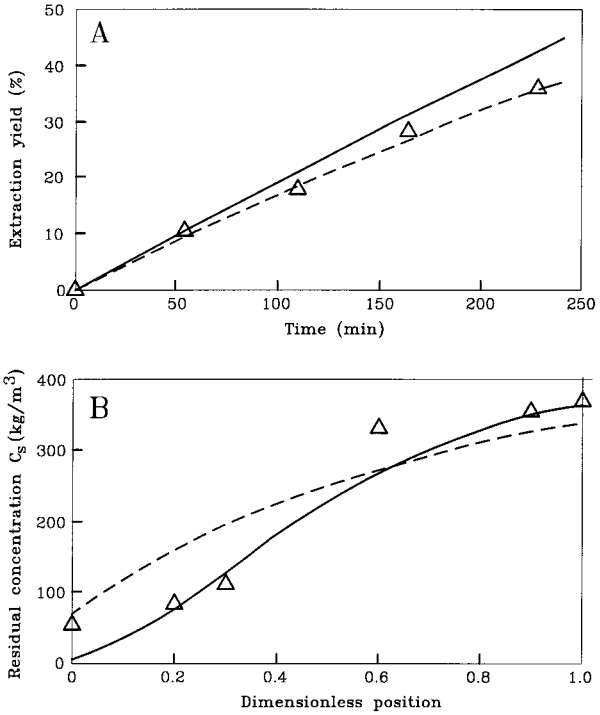

Figure 9. Fit of Model 2 to **(A)** integral extraction data and **(B)** residual concentration profile data reported by Lee et al.[12] for the extraction of oil from canola with supercritical carbon dioxide at 55 °C and 360 bar (Table 1). The fitting of external volumetric mass transfer coefficient ($k_f a_p$) was done using a single-objective procedure (utilizing only integral extraction data, segmented line) and a multi-objetive procedure (using both the integral extraction and residual concentration, continuous line). △ represents experimental data points.

confidence intervals when the multi-objetive procedure is used should not be considered as a disadvantage of the method. In fact, it is our impression that evident discrepancies between the experimental and simulated values of $C_s(z_k)$ when the single-objetive procedure is used are clear evidence of overadjustment caused by disregard of experimental evidence.

As a result of our simultation studies, we concluded that most proposed models for SFE processes predict similar, smooth integral extraction plots $Y(t)$, but may show important differences on $C_s(z)$ profiles. Thus, we suggest that a multi-objective fitting of experimental Y versus t curves as well as C_s versus z profiles be performed, so as to estimate relevant mass transfer parameters for SFE processes in packed substrate beds. We have not been able to retrieve our own $Y(t)$ and $C_s(z)$ experimental data yet to prove conclusively this point, and the manuscript by Lee et al.[12] did not provide us with all of the required information on extractor and particle geometry, and equilibrium between phases, to allow for a determination of mass transfer coefficients with full confidence. However, results obtained using Model 2 for the extraction of packed beds of crushed canola seeds show promise. This manuscript contributes some objective criteria that can be applied to neglect internal or external resistance to mass transfer in some selected cases: we can suggest neglecting one of them if its contribution to the total resistance is less than about 15%.

It is important to note that our base model is fairly simplistic in that it assumes an homogeneous solid substrate of spherical geometry and constant physical properties throughout the extraction process. Vegetable

substrates for SFE of fatty and essential oils have a cellular microstructure that has a considerable influence on extraction rates, and microstructural features are strongly affected by sample pretreatment (e.g., drying, milling, flaking, extrusion, and pelletization).[19] Pretreated substrate particles are seldom spherical in shape, and their relevant dimension (e.g., the thickness of flakes) may be different than that determined by sieving. Vegetable substrates are also constituted by many different solutes (e.g., volatile oils, free fatty acids, triglycerides, waxes, and heavy resins), which may be extracted concurrently at different rates that depend on their partition coefficients between the solid and fluid phase as well as on their locations within the substrate.[2,17] Finally, the porosity of the bed and specific surface of the particles change as a result of solute removal.[14] As a result of all of these factors, the mass transfer mechanism may switch from external to internal control during the process.[20] This emphasizes the need to expand this work using more detailed models for the extraction of solid substrates.

Acknowledgment

This work was financed by the Fund to Further the Scientific and Technological Development (FONDEF) of Chile through Research & Development Project D97I2026 ("Production of 'Premium' Extracts to be Used in Food and Related Industries") and by the National Fund of Science and Technology (FONDECYT) of Chile through Project 100-0382 ("Extraction of Densified Vegetables with Supercritical CO_2").

Nomenclature

a_p = specific surface of substrate particles [m^{-1}]
Bi = Biot's number [dimensionless]
C_f = solute concentration in SF phase [kg m^{-3}]
C_{fo} = solute concentration in SF phase at the beginning of the experiment [kg m^{-3}]
C_{fs} = solute concentration in SF phase at particle surface [kg m^{-3}]
C_s = solute concentration in solid phase [kg m^{-3}]
C_{so} = initial solute concentration in solid phase [kg m^{-3}]
$C_s|_R$ = solute concentration in the surface of the solid particle [kg m^{-3}]
$\bar{C}_s$ = average solute concentration in solid phase [kg m^{-3}]
$\hat{C}_s$ = estimated solute concentration in solid phase [kg m^{-3}]
d_e = diameter of cylindrical extractor [m]
D_m = diffusivity in solid phase [m^2 s^{-1}]
F = volumetric flow rate of SF [m^3 s^{-1}]
H = height of the bed [m]
J = amount of solute transferred from the solid to the fluid phase per unit bed volume [kg s^{-1} m^{-3}]
K = volumetric partition coefficient [dimensionless]
k_f = external mass transfer coefficient [m s^{-1}]
n = number of data points
p = number of fitting parameters
r = radial coordinate in the particle [m]
R = particle radius [m]
R_{ext} = external resistance to mass transfer [s]
R_{int} = internal resistance to mass transfer [s]
R_T = total resistance to mass transfer [s]
t = extraction time [s]
u = interstitial SF velocity [m s^{-1}]
x = dimensionless solute concentration in the solid phase
y = dimensionless solute concentration in the fluid phase
Y = extraction yield [%]
$\hat{Y}$ = estimated extraction yield [%]
z = distance to the entrance of the SF along the extractor [m]

Greek Letters

α = significance level of confidence interval
Δz = height of volume elements of the bed [m]
ϵ = void fraction in the bed [dimensionless]
Γ = dimensionless parameter
ν = degrees of freedom of Student's "t" probability distribution
θ = dimensionless time coordinate
Θ = dimensionless parameter (τ_{ext} K^{-1})
ρ = dimensionless radial coordinate within the particle
$\hat{\sigma}_Y$ = error standard deviation for measurements of recovered solute versus time
$\hat{\sigma}_{Cs}$ = error standard deviation for measurements of residual solute versus position
τ_{ext} = externally controlled characteristic extraction time [dimensionless]
τ_{int} = internally controlled characteristic extraction time [dimensionless]
ξ = dimensionless space coordinate along the packed bed
Ψ = dimensionless extraction yield

Literature Cited

(1) Williams, D. F. Extraction with Supercritical Gases. *Chem. Eng. Sci.* **1981**, *36*, 1769−1788.

(2) Brunner, G. *Gas Extraction. An Introduction to Fundamentals of Supercritical Fluids and the Application to Separation Processes*; Springer: New York, 1994.

(3) Bulley, N. R.; Fattori, M.; Meisen, A.; Moyls, L. Supercritical Fluid Extraction of Vegetable Oil Seeds. *J. Am. Oil Chem. Soc.* **1984**, *61*, 1362−1365.

(4) Cuperus, F. P.; Boswinkel, G.; Muuse, B. G.; Derksen, J. T. P. Supercritical Carbon Dioxide Extraction of *Dimorphotheca pluvialis* Oil Seeds. *J. Am. Oil Chem. Soc.* **1996**, *73*, 1675−1679.

(5) Roy, B. C.; Goto, M.; Hirose, T. Extraction of Ginger Oil with Supercritical Carbon Dioxide: Experiments and Modeling. *Ind. Eng. Chem. Res.* **1996**, *35*, 607−612.

(6) Goodarznia, I.; Eikani, M. H. Supercritical Carbon Dioxide Extraction of Essential Oils: Modeling and Simulation. *Chem. Eng. Sci.* **1998**, *53*, 1387−1395.

(7) Poletto, M.; Reverchon, E. Comparison of Models for Supercritical Fluid Extraction of Seed and Essential Oils in Relation to the Mass-Transfer Rate. *Ind. Eng. Chem. Res.* **1996**, *35*, 3680−3686.

(8) Reverchon, E. Mathematical Modeling of Supercritical Extraction of Sage Oil. *AIChE J.* **1996**, *42*, 1765−1771.

(9) Perrut, M.; Clavier, J. Y.; Poletto, M.; Reverchon, E. Mathematical Modeling of Sunflower Seed Extraction by Supercritical CO_2. *Ind. Eng. Chem. Res.* **1997**, *36*, 430−435.

(10) Reverchon, E.; Marrone, C. Supercritical Extraction of Clove Bud Essential Oil: Isolation and Mathematical Modeling. *Chem. Eng. Sci.* **1997**, *52*, 3421−3428.

(11) Goto, M.; Roy, B. C.; Kodama, A.; Hirose, T. Modeling Supercritical Fluid Extraction Process Involving Solute−Solid Interaction. *J. Chem. Eng. Jpn.* **1998**, *31* (2), 171−177.

(12) Lee, A. K. K.; Bulley, N. R.; Fattori, M.; Meisen, A. Modelling of Supercritical Carbon Dioxide Extraction of Canola Oilseed in Fixed Beds. *J. Am. Oil Chem. Soc.* **1986**, *63*, 921−925.

(13) Peker, H.; Srinivasan, M. P.; Smith, J. M.; McCoy, B. J. Caffeine Extraction Rates from Coffee Beans with Supercritical Carbon Dioxide. *AIChE J.* **1992**, *38*, 761−770.

(14) Eggers, R. Supercritical Fluid Extraction (SFE) of Oilseeds/Lipids in Natural Products. *Supercritical Fluid Technology in Oil and Lipid Chemistry*; King, J. W., List, G. R., Eds.; AOCS Press: Champaign, IL, 1996; pp 35−64.

(15) van Boekel, M. A. J. S. Statistical Aspects of Kinetics Modeling for Food Science Problems. *J. Food Sci.* **1996**, *61*, 477−485.

(16) Reverchon, E.; Donsi, G.; Sesti Osséo, L. Modeling of Supercritical Fluid Extraction from Herbaceous Matrices. *Ind. Eng. Chem. Res.* **1993**, *32*, 2721−2726.

(17) Reverchon, E. Supercritical Fluid Extraction and Fractionation of Essential Oils and Related Products. *J. Supercrit. Fluids* **1997**, *10*, 1−37.

(18) Tan, C. S.; Liang, S. K.; Liou, D. C. Fluid−Solid Mass Transfer in a Supercritical Fluid Extractor. *Chem. Eng. J.* **1988**, *38*, 17−22.

(19) Aguilera, J. M.; Stanley, D. W. *Microstructural Principles of Food Processing and Engineering*, 2nd ed.; Aspen Publishing, Inc.: Frederick, MD, 1999.

(20) Sovová, H. Rate of the Vegetable Oil Extraction with Supercritical CO_2. I. Modelling of Extraction Curves. *Chem. Eng. Sci.* **1994**, *49*, 409−414.

Received for review January 12, 2000
Revised manuscript received July 6, 2000
Accepted August 26, 2000

IE000034F